Desalination and Water Treatment
www.deswater.com

1944-3994 / 1944-3986 © 2011 Desalination Publications. All rights reserved.
doi: 10.5004/dwt.2011.2394

31 (2011) 59–63
July

Correlation of $CaCO_3$ induction times measured by an electrochemical technique

Irina Zaslavschi[a], David Hasson[a]*, Hilla Shemer[a] , Raphael Semiat[a], Mark Wilf[b], Craig Bartels[c]

[a]*Rabin Desalination Laboratory, Technion – Israel Institute of Technology, Haifa 32000, Israel*
Tel. +972 (4) 829-2936; Fax +972 (4) 8295672; email: hasson@tx.technion.ac.il
[b]*Consultant RO Technology, San Diego, CA, USA*
[c]*Hydranautics Oceanside, CA, USA*

Received 11 October 2010: Accepted 2 December 2010

ABSTRACT

Induction time data in $CaCO_3$ precipitation were determined by an electrochemical technique. The alkaline environment surrounding the cathode surface promotes $CaCO_3$ precipitation. The data were measured using simulated sea water solutions without the interfering presence of magnesium ions. The effect of current intensity on induction time was successfully correlated by a modified form of the classical nucleation equation. Data indicating the inception of precipitation by the first detectable decrease in solution concentration were also successfully correlated with a model based on population balance crystallization theory.

Keywords: $CaCO_3$ scale; Induction period; Electrochemical precipitation; Steady state nucleation; Population balance

1. Introduction

An induction time denotes the extent of the period between the creation of a supersaturated state in a salt solution and the moment when crystal formation is detected. The induction period phenomenon is of practical importance in scale control efforts. The present study is related to a problematic feature of the technique for minimizing the permeate boron content in sea water desalination. The pH level is raised so as to ensure high borate ion rejection. The elevated pH induces a high scaling potential and measures against scaling have to be taken. Induction time data can guide these measures.

Since the evolution of a scaling deposit can be lengthy, there is interest in short time tests that enable preliminary assessment of the scaling intensity. Electrochemical techniques have been proposed for rapid evaluation of scaling propensity. The alkaline scale deposits precipitating on the cathode surface have been used for characterizing scaling processes and for assessing the effectiveness of anti-scalants [1,2]. This paper presents an exploratory electrochemical study of induction times in $CaCO_3$ scale formation from sea water solutions.

2. Basis of the electrochemical tests

Scale forming species commonly encountered in different raw waters are calcium, magnesium and bicarbonate ions, all of which are prone to precipitation in an alkaline medium. An electrochemical cell provides an alkaline environment on the cathode surface by the hydrogen release reaction and the dissolved oxygen reduction [3]:

---

* Corresponding author.

Presented at EuroMed 2010 — Desalination for Clean Water and Energy: Cooperation among Mediterranean Countries of Europe and MENA Region, 3–7 October 2010, David Intercontinental Hotel, Tel Aviv, Israel. Organized by the European Desalination Society.

$$2H_2O + 2e^- \rightarrow H_2\uparrow + 2OH^- \tag{1}$$

$$O_2 + 2H_2O + 4e^- \rightarrow 4OH^- \tag{2}$$

The alkaline environment promotes precipitation of the calcium hardness in the form of $CaCO_3$ and of the magnesium hardness in the form of $Mg(OH)_2$:

$$Ca^{2+} + HCO_3^- + OH^- \rightarrow CaCO_3\downarrow + H_2O \tag{3}$$

$$Mg^{2+} + 2OH^- \rightarrow Mg(OH)_2\downarrow \tag{4}$$

3. Induction time models

An induction period involves two processes — formation of stable nuclei of critical size and crystal growth of the molecular size nuclei to a detectable magnitude. The induction time τ is therefore governed by the time t_N for the formation of critical nuclei and the time t_G for the growth process [4–6]:

$$\tau = t_N + t_G \tag{5}$$

When $t_N \gg t_G$, the induction period is determined primarily by the kinetics of critical nucleus formation [4]. A widely used correlating equation based on this premise is derived as follows. Assuming steady state nucleation, the nucleation rate J is given by:

$$J = A\exp\left[-\phi\frac{16\pi}{3}\frac{\sigma^3\upsilon_m^2}{v^2(k_BT)^3(\ln S_w)^2}\right] \tag{6}$$

where A is a frequency factor, σ is the surface energy of the nucleating surface, v_m is the molar volume of the solid, ν the number of ions per molecule ($\nu = 2$ for $CaCO_3$), T is absolute temperature, S_w is supersaturation ratio and k_B is the Boltzmann constant. The parameter ϕ has a limiting value of 1 for homogeneous nucleation (absence of a deposition surface) and a value of $\phi < 1$ which depends on the wetting angle for heterogeneous nucleation.

The induction period is taken to be inversely proportional to the nucleation rate [6]:

$$\tau = \frac{P}{J} \tag{7}$$

where P is a constant. Eqs. (6) and (7) provide an expression relating the induction period τ with the super saturation ratio S_w:

$$\ln\tau = \phi\frac{16\pi}{3}\frac{\sigma^3 v_m^2}{\upsilon^2(k_BT)^3(\ln S_w)^2} + \ln\frac{P}{A} \tag{8}$$

Eq. (8) has been found to apply in many systems. Values of the nucleation surface energy σ have been determined from the slope of the linear plot of $\ln\tau$ vs. $1/(\ln S_w)^2$ [7–11].

Söhnel and Mullin [4] proposed several elaborate models for the case of $t_N \sim t_G$. A rather simple model was derived by Hasson and Steinberg on the basis of the population balance crystallization theory [12]. The model takes into account the simultaneous processes of nucleation and crystal growth. The nucleation rate J and the linear crystal growth rate G are assumed to be power functions of the super saturation driving force ($C - C_s$), where C and C_s are solution and solubility concentrations respectively:

$$J = \frac{dN}{dt} = k_N\cdot(C - C_s)^i \tag{9}$$

$$G = \frac{dL}{dt} = k_g\cdot(C - C_s)^a \tag{10}$$

An experimental induction period depends on the measurement method since the inception of precipitation is determined from the first detectable change in some property such as solution conductivity, solution turbidity or solute concentration. For both plug flow and mixed flow conditions, the population balance model yields a simple expression relating induction time τ and initial precipitation rate $(-dC/dt)_{t=\tau}$ with the first detectable concentration change ΔC_D:

$$\tau\cdot\left(-\frac{dC}{dt}\right)_{t=\tau} = 4\cdot\Delta C_D = \text{const} \tag{11}$$

The first detectable concentration change ΔC_D is essentially the precision of the measurement method. Eq. (11) predicts that a plot of $\log\tau$ vs. $\log(-dC/dt)_{t=\tau}$ should yield a straight line having a negative slope of unity and y axis intercept of $\log[4\cdot\Delta C_D]$.

4. Experimental

Induction time data were measured in the electrochemical system shown in Fig. 1. The electrolytic cell consisted of a tubular anode (30 mm internal diameter, 100 mm long) and a central cylindrical cathode rod (16 mm diameter, 123 mm long). This configuration enabled clear observation of the scale depositing on the cathode. Both electrodes were made of a corrosion resistant titanium alloy. These so-called “dimensionally stable electrodes” (DSA) were supplied by Whizzo Science & Technology Co., China.

The test solution held in a 10 L feed vessel entered the bottom of the electrochemical cell and flowed in the 7 mm wide annular space between the electrodes. The flow rate of the solution was 5.5 L/min in all runs. Solution temperature was held constant at about 25°C.

The tests were carried out with artificial solutions of Pacific sea water having the composition listed in Table 1. Magnesium was omitted from the solutions in order to characterize induction times of $CaCO_3$ without the

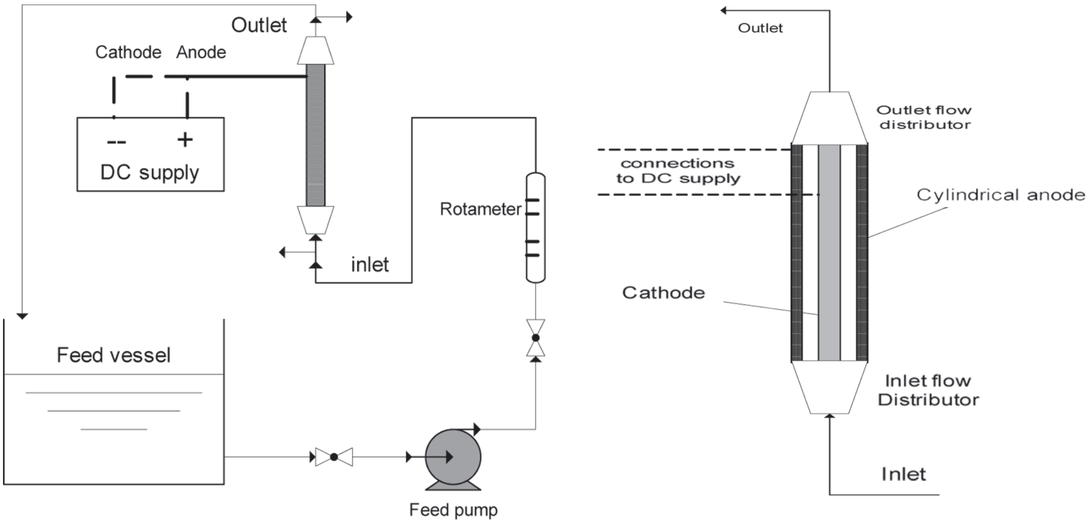

Fig. 1. Electrochemical precipitation system.

Table 1
Pacific seawater composition

Component	ppm
Ca^{2+}	356
Na^{+}	10669
Cl^{-}	18700
HCO_3^-	133
SO_4^{2-}	2500
pH	8.0
SI calcite	0.46

interfering influence of Mg ions. The experiments were performed at various current intensities in the range of 0.1–0.5 A, corresponding to current densities of 16–81 A/m^2. Each test was repeated at least twice.

Induction time data were derived from the periodic measurement of Ca^{2+} concentration in the recycling solution. Calcium concentrations were measured by EDTA titrations. The onset of precipitation was determined by the first detectable change in calcium concentration. The titrations were performed using a burette of 0.05 ml precision and an EDTA concentration of 0.002 M. Two sets of experiments were carried out differing in the sample volume taken for analysis from the recycling solution. The sample volume was 2 mL in the first experimental set and 4mL in the second experimental set. These data show that the precision in the first experimental set was $\Delta Ca = 2$ ppm and in the second, $\Delta Ca = 1$ ppm.

Fig. 2 shows a typical plot of calcium concentration vs. time used for determining the induction time and the initial slope.

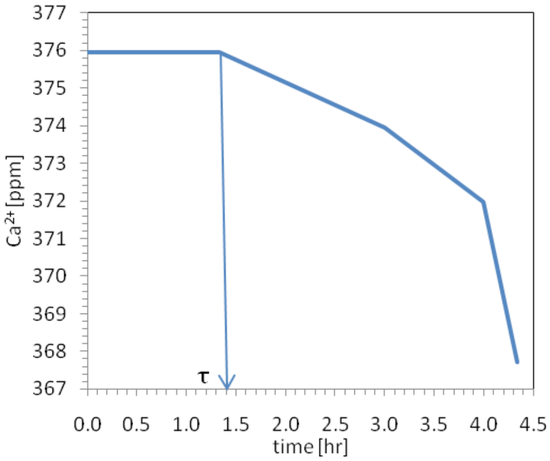

Fig. 2. Typical plot of the change in time in the Ca^{2+} content of the recycling solution (current density of 16.2 A/m^2).

5. Analysis of induction time data

5.1. Current density correlation

Fig. 3 displays measurements of induction time and of average $CaCO_3$ precipitation rates obtained at different current densities. The experimental data show the expected trends of shortened induction times and enhanced precipitation rates at increasing current densities. The increase in current density induces a higher evolution of OH^- on the cathode surface according to Faraday's law:

$$J_{OH^-} = \frac{i}{F} \tag{12}$$

where J_{OH^-} is the flux of hydroxyl ions, i is the current density and F is the Faraday constant. Higher alkaline

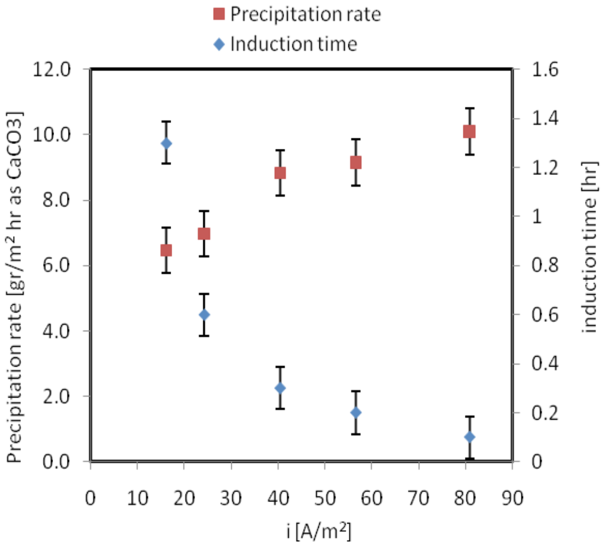

Fig. 3. Effect of current density on the induction time and precipitation rate of $CaCO_3$.

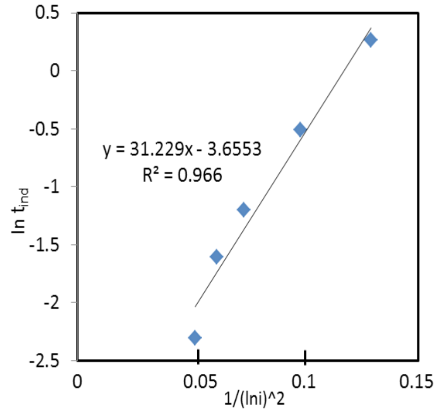

Fig. 4. Linear correlation of induction time with current density.

levels on the cathode surface augment the super saturation ratio of $CaCO_3$ and act to reduce the induction time

The induction time correlation described by Eq. (8) was tested by assuming that the supersaturation ratio S_w is proportional to the current intensity i:

$$\ln\tau \propto \phi \frac{16\pi}{3} \frac{\sigma^3 v_m^2}{\upsilon^2 (k_B T)^3 (\ln i)^2} + \ln\frac{P}{A} \qquad (13)$$

Eq. (13) predicts a linear correlation between ln τ and $1/(\ln i)^2$. The data plotted in Fig. 4 show that the expected linear correlation is observed. This suggests that Eq. (13) can serve to correlate electrochemical induction time measurements.

5.2. Induction time and initial precipitation rate correlation

As described in Section 4, Eq. (11) was tested by data measured in two sets of experiments, one performed with a precision of 2 ppm Ca^{2+} and the other with a precision of 1 ppm Ca^{2+}. Fig. 5 shows that for both experimental sets, the linearity in the plots of log τ vs. $\log(-dC/dt)_{t=\tau}$ predicted by the model is observed. Analysis of the experimental relations, shown in Table 2, indicates that they conform closely to model predictions. The slopes of the lines are near the anticipated value of unity and the experimental values of $[\Delta C_D]$ of 1.7 and 0.87 ppm are close to the predicted values of 2 and 1 ppm respectively.

5. Concluding remarks

Results of this exploratory study indicate that electrochemically determined $CaCO_3$ induction time data can be successfully analyzed according to two models. The relation between induction time and current intensity may be correlated using a modified form of the classical nucleation model. Detection of the inception of precipitation from the change in solution properties can be correlated by the population balance model which takes into account both the process of nucleation and of crystal growth. Further work is being undertaken with different

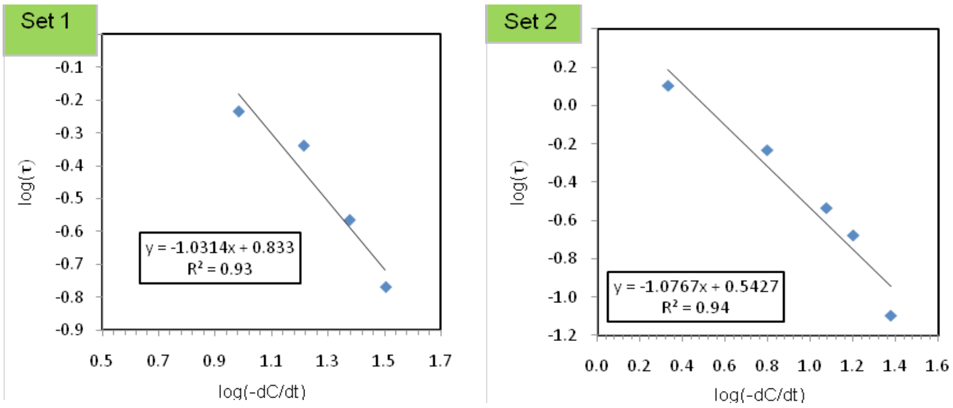

Fig. 5. Plots of induction time vs. initial precipitation rate.

Table 2
Comparison of experimental results with predicted values

Set 1: 2 ml sample for EDTA titration	Set 2: 4 ml sample for EDTA titration
$\log(\tau)+1.0314\cdot\log\left(-\frac{dC}{dt}\right)=0.833$ $\tau\cdot\left(-\frac{dC}{dt}\right)_{t=\tau}^{1.0314}=4x\underbrace{1.7}_{\Delta C_D}$	$\log(\tau)+1.0767\cdot\log\left(-\frac{dC}{dt}\right)=0.5427$ $\tau\cdot\left(-\frac{dC}{dt}\right)_{t=t^0}^{1.0767}=4x\underbrace{0.87}_{\Delta C_D}$
$\Delta C_D=1.7\approx 2\,\mathrm{ppm\ Ca}$	$\Delta C_D=0.87\approx 1\,\mathrm{ppm\ Ca}$

precipitation systems in order to verify the applicability of the exploratory results to other systems.

References

[1] C. Gabrielli, M. Keddam, H. Perrot, A. Khalil, R. Rosset and M. Zidoune, Characterization of the efficiency of anti-scale treatments of water. Part I: Chemical processes, J. Appl. Electrochem., 26 (1996) 1125–1132.

[2] C. Gabrielli, G. Maurin, G. Poindessous and R. Rosset, Nucleation and growth of calcium carbonate by an electrochemical scaling process, J. Crystal Growth, 200 (1999) 236–250.

[3] D. Hasson, V. Lumelsky, G. Greenberg, Y. Pinhas and R. Semiat, Development of the electrochemical scale removal technique for desalination applications, Desalination, 230 (2008) 329–342.

[4] O. Söhnel and J.W. Mullin, Interpretation of crystallization induction periods, J. Colloid Interface Sci., 123 (1988) 43–50.

[5] O. Söhnel and J. Garside, Precipitation: basic principles and industrial applications, Butterworths-Heinemann, Oxford, 1992.

[6] J.W. Mullin, Crystallization, 4th ed., Butterworths-Heinemann, Oxford, 2001.

[7] H. Roques and H.A. Girou, Kinetics of the formation conditions of carbonates tartars, Water Res., 8 (1974) 907–920.

[8] O. Söhnel and J.W. Mullin, A method for the determination of precipitation induction periods, J. Crystal Growth, 44 (1978) 377–382.

[9] O. Söhnel and J.W. Mullin, Precipitation of calcium carbonate, J. Cryst. Growth, 60 (1982) 239–250.

[10] W. Wu and G.H. Nancollas, Determination of interfacial tension from crystallization and dissolution data: a comparison with other methods, Adv. Colloid Interf. Sci., 79 (1999) 229–279.

[11] D. Hasson, A. Drak and R.Semiat, Induction times induced in an RO system by anti-scalants delaying $CaSO_4$ precipitation, Desalination, 157 (2003) 193–207.

[12] D. Hasson and S. Steinberg, Continuous flow precipitation, Desalination, 47 (1983) 129–148.